Surface Science 605 (2011) 1202–1208

Contents lists available at ScienceDirect

Surface Science

journal homepage: www.elsevier.com/ locate/susc

DFT study of isocyanate chemisorption on Cu(100) Correlation between substrate–adsorbate charge transfer and intermolecular interactions

Patricia G. Belelli [a,*], Graciela R. Garda [a], Ricardo M. Ferullo [a,b]

[a] Grupo de Materiales y de Sistemas Catalíticos, Departamento de Física, Universidad Nacional del Sur, Av. Alem 1253, Bahía Blanca, B8000CP, Argentina
[b] Departamento de Química, Universidad Nacional del Sur, Av. Alem 1253, Bahía Blanca, B8000CP, Argentina

ARTICLE INFO

Article history:
Received 4 January 2011
Accepted 2 April 2011
Available online 8 April 2011

Keywords:
Adsorption
NCO
Copper
Work function
Dipole moment

ABSTRACT

The adsorption of isocyanate (−NCO) species on Cu(100) was studied using the density functional theory (DFT) and the periodic slab model. The calculations indicate that at low and intermediate coverages NCO adsorbs preferentially on bridge and hollow sites. Work function and dipole moment changes show a significant negative charge transfer from Cu to NCO. The resulting charged NCO species interact repulsively among themselves being these dipole–dipole interactions particularly intensive when they are adsorbed in adjacent sites. Consequently, isocyanates tend to be separated from each other generating the vacant sites required for the dissociation to N and CO. This condition for NCO dissociation has been suggested in the past from experimental observations. A comparison was also performed with the NCO adsorption on Pd(100). In particular, the calculated minimal energy barrier for NCO dissociation was found to be higher on Cu(100) than on Pd(100) in accord with the well known higher NCO stability on Cu(100).

1. Introduction

Isocyanate species (−NCO) is formed during the catalytic reduction of nitrogen oxides in the presence of CO or hydrocarbons. Infrared spectroscopy (IR) measurements performed on metal-supported catalysts show that NCO is produced on the metal and then migrates onto the support where it is accumulated and stabilized [1–3]. Besides, it can be the source for the formation of undesirable contaminants such as HCN, C_2N_2, NH_3 and HNCO [4,5].

The adsorption of NCO over well-defined metal faces has been used to understand its surface chemistry at a fundamental level. Since it is very difficult to produce NCO over pure metals via NO + CO reaction, the dissociative adsorption of isocyanic acid (HNCO) has been used as a source of surface NCO. In particular, it was observed that HNCO interacts in a very different way on the (111) and (100) faces of Cu. Solymosi and Kiss found that HNCO does not adsorb at 300 K on Cu(111) but readily reacts with preadsorbed oxygen to give surface NCO [6], which is stable up to 400 K. More recently, Celio et al. investigated NCO adsorption on Cu(100) from thermal decomposition of HNCO at 300 K and from the reaction of cyanogen (C_2N_2) with preadsorbed oxygen [7]. The NCO obtained from both methods was stable on this surface up to 500 K. On Pd(100), NCO (also generated from HNCO) totally decomposes at lower temperatures (about 300 K) [8]. On Pt(111) and Pt(110) [9,10], HNCO adsorbs molecularly at very low temperatures and decomposes at about 250 K to form CO and atomic N without forming stable isocyanate species.

In the available published literature there are only a few theoretical studies about NCO adsorption on well-defined transition-metal surfaces [11–15]. The NCO decomposition toward atomic N and CO was found to be about 1 eV on Pd(111) using a semi-empirical molecular orbital method [12]. Moreover, the adsorption of NCO species on Ni(100) [11] and on Cu(100) [13,14] was studied by cluster models and ab initio calculations. The results showed that for both surfaces, hollow and bridge sites are the most favored. When NCO adsorbs on Cu(100), an asymmetric mode at 2187 cm^{-1} was predicted for the fourfold site [13] and the calculated symmetric and asymmetric NCO stretching frequencies are all blue-shifted compared to the values of free NCO [14], in agreement with the experimental evidence. In a previous work, the preference to adsorb at high coordination sites was also found on Pd(100) [15] using a periodic slab model. Besides, work function and dipole moment calculations evidence an important charge transfer from the metal surface to NCO [14,15]. Theoretical approaches predict that the isocyanate complex adopts a lineal and perpendicular configuration with respect to the surface, linking through the N atom [11,14]. In addition, other molecular orbital studies concerning NCO adsorption on Cu aggregates [16] and on silica-supported Cu particles showed a large charge transfer from the metal to NCO [17].

* Corresponding author. Tel.: +54 291 4595141; fax: +54 291 4595142.
E-mail address: pbelelli@plapiqui.edu.ar (P.G. Belelli).

0039-6028/$ – see front matter © 2011 Elsevier B.V. All rights reserved.
doi:10.1016/j.susc.2011.04.002

It was established that NCO adsorbed on Pt(100) requires vicinal vacant sites for its decomposition to surface CO and N:

$$NCO(ads) + site \rightarrow CO(ads) + N(ads).$$

This conclusion was attained because the stability of NCO is enhanced at high CO coverage on Pt(100); besides, when a small amount of CO desorbs by heating, a few vacant sites are created triggering immediately the dissociation of NCO. On Rh(111), preadsorbed oxygen enhances the NCO stability region at least by 60 K [18]. In this latter case, it was suggested that O preadsorbed atoms could block sites for the formation of the dissociation products, CO (ads) and N (ads). Similar effect of preadsorbed O was recently observed on Pd(100) [8].

In our previous work performed on NCO/Pd(100) we observed that at high coverage the bond strength between NCO and the surface was relatively weak owing to strong lateral repulsion among isocyanates. This intermolecular interaction is in turn produced by a substantial electronic charge transfer from the surface to NCO yielding intensive dipole–dipole repulsive interactions. Therefore, as a general tendency, NCO prefers to be separated from each other to minimize lateral repulsions. This behavior could have a direct relation with the abovementioned requirement of free vicinal sites to facilitate surface dissociation. In this work we investigate the adsorbate–substrate charge transfer for the NCO/Cu(100) interface, its dependence with the coverage and adsorption site, the nature of the NCO–NCO interactions and the possible correlation between the intermolecular interactions and the NCO dissociation.

2. Computational details

The calculations performed in this work were carried out in the framework of DFT using the *Vienna* Ab initio *Simulation Package* (VASP) [19–21]. Plane wave basis sets were used to solve the Kohn–Sham equations. The electron–ion interactions were described by the projector-augmented wave method (PAW). The PAW method is a frozen core all-electron method that uses the exact shape of the valence wave functions instead of pseudo-wave functions [22,23]. Electron exchange and correlation effects were described by the generalized gradient approximation (GGA), using the functional described by Perdew and Wang (PW91) [24,25].

The fixed convergence of the plane-wave expansion was obtained with a cutoff energy of 311 eV. Previously, it was checked that the increasing of the cutoff up to 600 eV does not change the total energies by more than 0.009 eV/atom. The two dimensional Brillouin integrations were performed on a grid of $7\times7\times1$ Monkhorst–Pack special *k*-points for the 1×1 and 2×2 cells, and of $3\times3\times1$ *k*-points for the 3×3 supercell [26]. In all the cases, a Methfessel–Paxton smearing of width $\sigma=0.2$ eV was used and the reported total energies were then extrapolated to $\sigma\rightarrow0$ eV [27]. Optimized geometries were found when the forces on atoms were smaller than 0.01 eV/Å.

The Cu(100) surface was represented with a slab containing four atomic metal layers. The effect of the slab thickness was tested considering slabs including up to 6 atomic layers. The results showed that a slab with four layers provides converged results, with accuracy of about 0.04 eV. Therefore, a slab with four atomic layers should be appropriate to the present study. A three dimensional periodic cell was constructed including a vacuum gap of ~13 Å in the perpendicular direction to the metallic surface. The thickness of this vacuum region was found to be adequate to eliminate any interaction between adsorbed molecules on adjacent metal slabs.

The lattice constant for the fcc Cu crystal cell parameter was optimized for the bulk structure, giving a value of 3.636 Å, which is about 0.7% larger than the experimental value (3.61 Å [28]). Thus, the Cu – Cu interatomic distance was 2.574 Å for bulk structure. The bulk modulus was calculated by varying the cell volume around the equilibrium value and fitting the Murnaghan equation of state. The value was estimated to be 136 GPa, in excellent agreement with the experimental value (137 GPa) [28] and with DFT calculations performed by Da Silva et al. (138 GPa) [29].

In the Cu(100) surface, the two uppermost layers were allowed to relax completely together with the NCO species. The other two metal layers were maintained fixed at the bulk geometry. For the bare copper surface, a contraction of −3.3% and a slight expansion of +0.3% were observed for the Δd_{12} and Δd_{23} interlayer distances, respectively, in comparison with the bulk interlayer distances. These results are in agreement with several computational and experimental results that showed the same trend, namely, a contraction of Δd_{12} and an expansion of Δd_{23} with a greater change in the surface contraction. While theoretical values vary in the range of −6.2 to −2.1% for Δd_{12} and +1.0 to +0.7% for Δd_{23}[29–32], the corresponding intervals obtained from experimental measurements are −3.0 to −1.0% and +2.0 to +0.1%, respectively [33,34].

There are three possible high-symmetry binding sites for NCO species on the Cu(100) surface: on-top, twofold bridge and fourfold hollow. Each adsorption site was evaluated on the (1×1), $c(2\times2)$, $p(2\times2)$ and $p(3\times3)$ cells, which correspond to the coverages of 1.0, 0.5, 0.25 and 0.11 ML (monolayer), respectively (see Fig. 1). The adsorption energy (E_{ads}) was calculated as the difference between the energy of the adsorbed system ($E_{NCO/Cu}$) and the sum of the free surface (E_{Cu}) and the gas-phase molecule (E_{NCO}) energies accordingly to the following equation:

$$E_{ads} = E_{NCO/Cu} - E_{Cu} - E_{NCO}$$

Negative values indicate exothermic chemisorption processes.

Given the large separation between two nearby NCO at the lowest coverage, $\theta=0.11$ (about 7.7 Å), the mutual effect among NCO can be considered insignificant, and therefore the magnitude of adsorption energy (E_{ads}) measures the interaction between NCO and the Cu(100) surface. We thus define the difference between E_{ads} at the higher coverages and that corresponding to the lowest coverage:

$$\Delta E_{ads} = E_{ads}(site, \theta \geq 0.25) - E_{ads}(site, \theta = 0.11).$$

Therefore, ΔE_{ads} can be considered as a direct measure of the effect of approaching surface NCO species on the NCO–metal interaction.

The vibrational frequencies were performed to validate the true potential energy minima and they were calculated considering a harmonic approach. The corresponding Hessian dynamical matrix was calculated by a finite difference method where the atoms in the NCO molecule were independently displaced by ±0.015 Å along each Cartesian coordinate direction. Afterwards, the harmonic molecular frequencies were obtained by a diagonalization of the Hessian dynamical matrix. Finally, the stretching frequencies were corrected with a scaling factor of 0.9823. This value was calculated through a least-squares procedure [35], considering the calculated and experimental stretching frequencies of free NCO species [36].

The electronic structure of the NCO/Cu interaction was analyzed by calculating the local density of states (LDOS) at selected atoms. The change of the work function ($\Delta\Phi$) was obtained as the difference between the work function of the surface with and without adsorbed NCO. The work function itself was obtained by computing the electrostatic potential of the corresponding surface. The calculated work function of the clean surface was 4.58 eV, in very good agreement with the experimental result (4.59 eV, [37]). The dipole moment (μ) was also evaluated by numerical integration of charge densities over the entire cell from a single point energy calculations on relaxed structures, as implemented in VASP. The dipole moment values and their changes were reported per one NCO species. This vector was considered as positive from the positive to the negative charge. In our case, by symmetry only the component normal to the surface is not null.

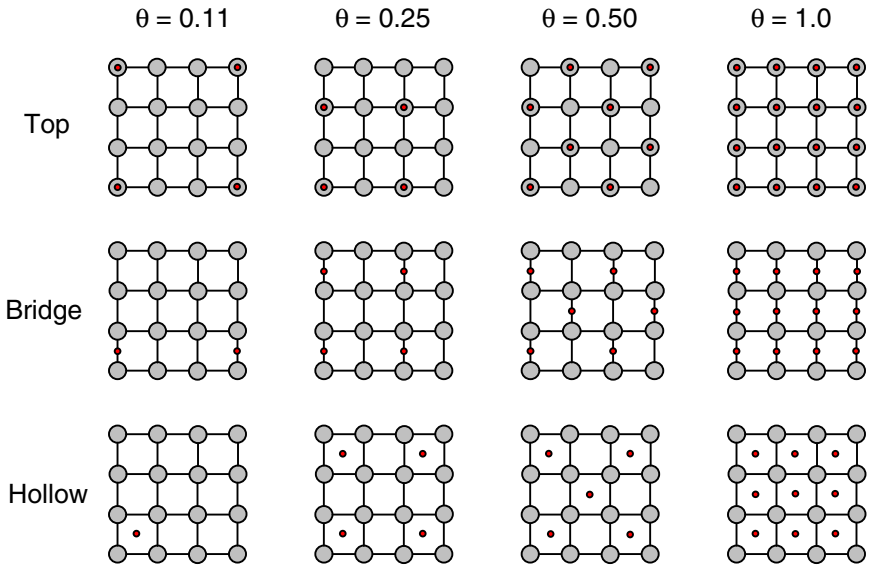

Fig. 1. Schematic representation of the different coverages for adsorbed NCO on the Cu(100) surface.

3. Results and discussion

The values of adsorption energies presented in Table 1 show a strong interaction between NCO and Cu(100). Excepting for complete coverage, the adsorption energies are in the range of −2.9 to −3.4 eV. NCO adsorbs in all the cases perpendicular to the surface with N-metal distances between 1.82 and 2.22 Å, depending on the adsorption site. The N–Cu distance increases as the site coordination number increases, and its variation is more pronounced than that corresponding to the NCO intramolecular distances. Besides, at each coverage, N–C and C–O distances present an opposite tendency; while the N–C distance increases the C–O bond decreases by going from the top to the hollow site. The explanation of this behavior was thoroughly developed in our previous work concerning the NCO adsorption on Pd (100) [15]. The 2π MO of NCO (occupied by one electron at free state), has a N–C bonding character and a C–O antibonding character. Upon adsorption, this MO mixes strongly with the metal band gaining electronic charge and hence producing opposite effects on the N–C and C–O bonds. Thus, this behavior should be consistent with the amount of electronic charge taken by NCO according to the adsorption sites. The NCO charge should vary following the sequence top>bridge>hollow that is precisely the order obtained using Cu clusters according to the Hirshfeld population analysis [13]. Considering all the studied situations, the N–C and C–O distances vary in the ranges of 1.210–1.240 Å and 1.180–1.197 Å, i.e., around the corresponding values at the free isocyanate species (d(N–C) = 1.231 Å and d(C–O) = 1.194 Å). Comparing these results with those previously obtained on Pd(100), we observe that the N–Cu distances are approximately 0.1 Å shorter than the N–Pd ones [15].

In Fig. 2 the variation of NCO adsorption energies for the different sites as a function of the coverage is presented. For each site, the adsorption energy values have a nearly constant value up to 0.5 ML. The values corresponding to the on-top sites are significantly lower than on the other sites. NCO adsorbs preferentially on high coordination sites (bridge and hollow) irrespective of the coverage, excepting at θ = 1.0. At complete coverage, the destabilization on bridge and hollow adsorption sites increases abruptly reaching ΔE_{ads} values of about 2 eV (Table 1) indicating very strong intermolecular interactions. The top site is the less affected by the NCO–NCO repulsion with a ΔE_{ads} value of approximately 1.7 eV. For θ = 1.0 the bridge adsorption site is still the most stable one, with an energy difference with respect to the hollow site of 0.16 eV. The energy values indicate a stronger adsorption of NCO on Cu(100) than on Pd(100) [15]. Indeed, on Cu(100) the adsorption is around 0.5 eV stronger at coverages lower than 0.5 ML; yet at complete coverage the adsorption is slightly more stable on Pd(100) possibly due to its more open structure.

The effect of the metal surface on the NCO–NCO interaction was evaluated considering the energy difference between the non-adsorbed NCO layers at the N–N distance of 2.57 Å (equivalent to the N–N distance when the NCO is adsorbed on Cu surface at a coverage of θ = 1.0) and at the N–N distance of 7.72 Å (equivalent to the N–N distance when the NCO is adsorbed on Cu surface at coverage of

Table 1
Adsorption energies (E_{ads}, eV), adsorption energy differences (ΔE_{ads}, eV), work function ($\Delta\Phi$, eV), optimized distances (Å), and NCO frequencies (ν, cm^{-1}) for NCO chemisorption on Cu(100) at different coverages.

Coverage	θ = 0.11			θ = 0.25			θ = 0.5			θ = 1.0		
Sites	Top	Bridge	Hollow	Top	Bridge	Hollow	Top	Bridge	Hollow	Top	Bridge	Hollow
E_{ads}[a]	−3.01	−3.40	−3.35	−2.91	−3.37	−3.31	−2.78	−3.25	−3.23	−1.32	−1.47	−1.31
ΔE_{ads}[b]	0.00	0.00	0.00	0.10	0.03	0.04	0.23	0.15	0.12	1.69	1.93	2.04
$\Delta\Phi$	1.70	1.00	0.51	2.73	1.75	1.02	3.78	2.87	1.88	3.36	3.10	2.92
d(N–C)	1.210	1.222	1.239	1.214	1.225	1.240	1.216	1.227	1.240	1.212	1.218	1.229
d(C–O)	1.197	1.188	1.183	1.192	1.185	1.181	1.187	1.183	1.181	1.189	1.183	1.180
d(N–Cu)	1.854	1.983	2.223	1.845	1.970	2.212	1.822	1.964	2.215	1.881	1.978	2.207
ν(N–C–O)[c]	2172	2155	2115	2189	2182	2140	2230	2226	2179	2114	2171	2171
ν(N–C–O)[d]	1312	1279	1222	1321	1282	1221	1338	1284	1225	1309	1286	1246

[a] $E_{ads} = E_{NCO/Cu100} - E_{Cu100} - E_{NCO}$.
[b] $\Delta E_{ads} = E_{ads}(\text{site}, \theta \geq 0.25) - E_{ads}(\text{site}, \theta = 0.11)$.
[c] Asymmetric stretching mode.
[d] Symmetric stretching mode.

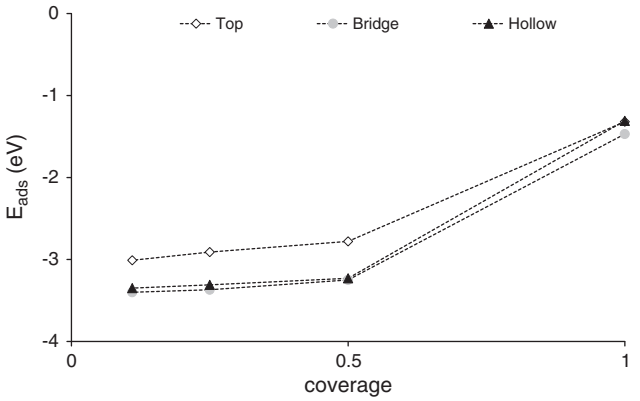

Fig. 2. Adsorption energies (in eV) of NCO species on Cu(100) at different adsorption sites as a function of the NCO coverage.

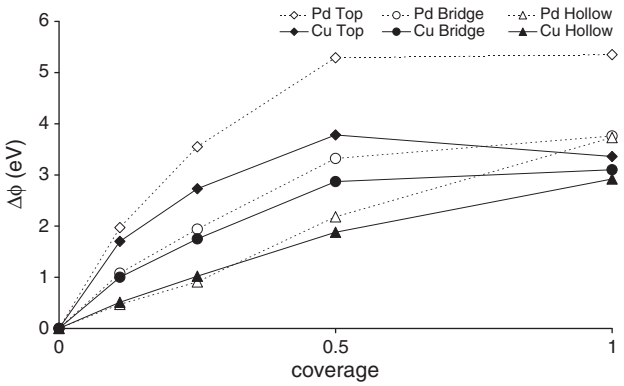

Fig. 4. Work function changes (in eV) as a function of NCO coverage for: NCO/Cu(100) (solid lines) and NCO/Pd(100) (dashed lines).

θ = 0.11). This energy difference is very small (−0.02 eV) showing that essentially there is no interaction among free parallel NCO even when they are very close. However, the situation is very different when NCO is adsorbed on Cu(100) as we have already observed from ΔE_{ads} values (see Table 1). This behavior can be associated with the repulsive interaction among isocyanates due to the significant electron charge gained by the NCO species when they are adsorbed on Cu, as it will be explained in the following paragraphs.

The dipole moment change, Δμ, was calculated as the difference between μ of the NCO/Cu(100) system and that of the bare Cu(100) surface. In Fig. 3 the values for the different sites and NCO coverages are shown, together with the results for the adsorption on Pd(100) previously reported [15]. Although different effects contribute to the dipole moment change, the Δμ values evaluated by this single difference can be considered as a direct measure of the adsorbate–substrate electronic charge transfer, as it was discussed in detailed in Ref. [15]. The positive values of Δμ indicate the direction of the electronic transfer: from Cu to NCO. For each value of coverage (excepting the complete saturation) Δμ values follow the order top>bridge>hollow, in line with the tendency in the NCO charges previously deduced from the variations in the internal distances. On the other hand, for each site the coverage dependence is different. While for the hollow site the values are practically the same over all the range of coverage, for bridge and top sites a continuous decreasing of Δμ is observed as the NCO – NCO distance decreases. With increasing coverage, an intermolecular repulsion occurs among charged NCO species. To reduce this repulsion, on top and bridge sites some partial electron charge is transferred back to the surface resulting in a depolarization. At θ = 1.0 ML, Δμ have practically the same values. The general behavior is similar on Pd(100)

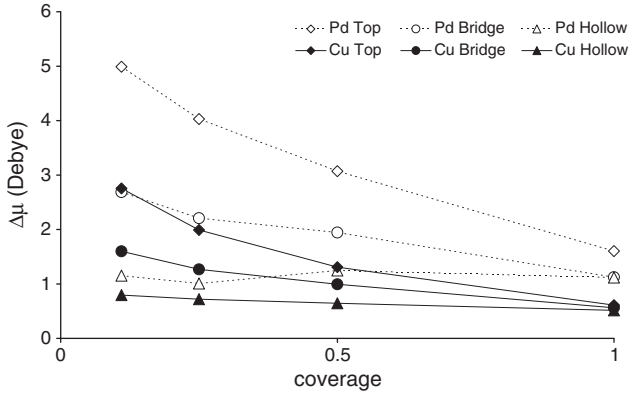

Fig. 3. Dipole moment changes (in Debye) as a function of NCO coverage for: NCO/Cu(100) (solid lines) and NCO/Pd(100) (dashed lines).

but, for each type of site, Δμ values are larger on this metal surface indicating a higher electronic charge transfer than on Cu.

Taking into account that the work function (Φ) is a sensitive property of the surface, we evaluate its change (ΔΦ) with respect to the bare Cu(100) surface for different adsorption sites and NCO coverages. Positive values of ΔΦ indicate the presence of negative charged adsorbates; in this case, a positive image charge is formed into the metal giving rise to a dipole layer which the emitted electron must pass through. The values of ΔΦ are presented in Table 1 and Fig. 4. In general, for each value of coverage, the magnitude of ΔΦ follows the order: top>bridge>hollow, i.e., the expected tendency taking into account the calculated Δμ values. For the three adsorption sites, ΔΦ values show an increasing behavior from θ = 0.11 to 0.5. In particular for the hollow site, a linear dependence along the whole range is observed. In this case, the successive incorporation of NCO increases the density of the induced dipoles and consequently ΔΦ becomes a linear function of the coverage. On the other hand, the non-linear behavior for top and bridge sites can be explained by the coverage dependent charge transfer between Cu and NCO. In these cases, the dipole–dipole interaction produces an increasing depolarization effect as the coverage increases. Particularly in going from 0.5 to 1.0 ML the more compact dipole layer is counterbalanced by the depolarization and as a consequence ΔΦ does not change. The same general behavior was previously reported for NCO/Pd(100) [15] and, for comparison their ΔΦ values are included in Fig. 4. For each site, the ΔΦ are lower on Cu(100) indicating a minor effort to extract an electron from the NCO/Cu(100) system, in agreement with the lower charge transfer from Cu to NCO predicted from the reported Δμ values.

On the other hand, the NCO/Cu(100) electronic structure was analyzed by means of the local density of states (LDOS) for Cu (d-orbitals) and N (p-orbitals). In Fig. 5 the LDOS for the NCO adsorbed on top, bridge and hollow on Cu(100) at θ = 0.11 are plotted. The energies are referred to the Fermi level. Four different set of features appear for N orbitals at low, medium and high energies, corresponding to different MOs of NCO. The inner peak between −17 and −19 eV corresponds to the N-p contribution of 6σ MO of NCO. A displacement to higher energies is observed as the coordination number decreases owing to a greater electronic charge transfer taken by NCO when it is adsorbed on top site. This site-dependence of charge transfer is supported by the analysis of the work function change and the dipolar moments discussed above. The same displacement was observed in the bands associated with 7σ, 1π and 2π MOs of NCO [13]. The 7σ MO appears as a double peak at −7.4 and −6.2 eV for top site, and moves to lower energies at −9.0 and −7.7 eV for hollow site. The 1π MO is located at −5.4 eV for top and −7.1 eV for hollow site. The 2π MO (as a double peak) overlaps with the upper part of the d-band on top, and with the bottom part of the band on hollow.

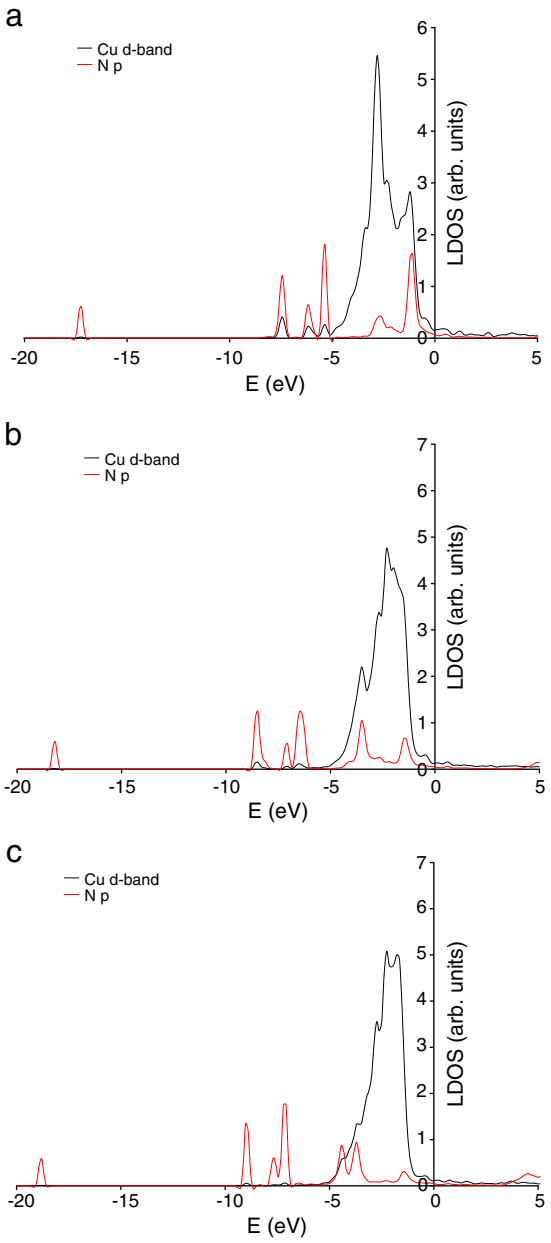

Fig. 5. LDOS localized on N and Cu atoms for NCO/Cu(100) at θ = 0.11 on: (a) top; (b) bridge and (c) hollow.

A vibrational frequency analysis was done for all the coverages and adsorption sites (Table 1). Two characteristic bands at about 2200 and 1300 cm^{-1} are observed, corresponding to the asymmetric and symmetric stretching modes of NCO, respectively. For $\theta \leq 0.5$ both NCO stretching frequencies decrease in the order: $\nu_{top} > \nu_{bridge} > \nu_{hollow}$. The same order was obtained in a previous work using cluster models [13]. Besides, for each site and also for $\theta \leq 0.5$, the frequency values increase as the NCO coverage increases. The calculated shift resulted to be in the range of 60–70 cm^{-1}, very similar than the displacement experimentally measured from low HNCO exposure to the one corresponding to the saturated limit [7]. However, the calculated asymmetric NCO frequency values present a general drop at θ = 1.0, not observed by Celio et al. This fact could be interpreted that the complete coverage, i.e., having one NCO per Cu atom, is not possible to achieve due to the strong intermolecular interactions. On the other hand, for each value of coverage, as the frequency values increase, the N–C distances decrease, i.e., $d(N-C)_{top} < d(N-C)_{bridge} < d(N-C)_{hollow}$ and, at the same time, the C–O distances increase. Moreover, the changes in the N–C bonds are greater than in the C–O bonds, namely, about 0.03 Å and 0.01 Å, respectively. Thus, the variation of the N–C bond seems to be the main factor that governs the asymmetric vibrational frequency values of NCO.

The experimental results obtained by Celio et al. [7] showed that NCO species can be formed from HNCO exposure on Cu(100), and by exposing cyanogen on oxygen precovered Cu(100). An interesting fact was the different relationship between NCO asymmetric frequency values and NCO coverage with (HNCO or C_2N_2) exposure. For both cases, the limiting values of coverage (obtained from the peak area) were reached at about 150 L, but the NCO coverage formed from HNCO was higher than twice that obtained from C_2N_2/O. Besides, at the corresponding high coverage limit, the frequency was 2227 cm^{-1} from HNCO and 2199 cm^{-1} from C_2N_2/O. As it was discussed in that article, the difference in the frequencies could not be explained only assuming that a higher NCO coverage was achieved from HNCO exposure [7]. This situation is clearer by comparing the frequencies for a same value of NCO coverage. For example, for a HNCO exposure that gives the same peak area as the highest peak area achievable from C_2N_2/O reaction, the value is about 2180 cm^{-1} from HNCO and about 2201 cm^{-1} from C_2N_2/O. Thus, the authors suggest that unreacted adsorbed oxygen should remain on the surface along with the NCO produced by the cyanogen reaction, and this unreacted oxygen could influence the frequency dependence on coverage. To add some support to these observations, we performed a theoretical modeling as follows, considering two situations with the same NCO coverage. At the experimental conditions followed by Celio et al. the oxygen precovered surface yields a c(2×2) pattern corresponding to a coverage of 0.5 ML. If we assume that half of the O reacts to form NCO, we have a final situation with θ(O) = 0.25 and θ(NCO) = 0.25. We modeled this surface structure with NCO at bridge sites and O at hollow sites (the distance between the N of NCO and the O is about 2.9 Å). The calculated NCO stretching frequency resulted to be 2190 cm^{-1}, a higher value than that for θ(NCO) = 0.25 ML in a p(2×2) array on bridge site but without adsorbed oxygen (2182 cm^{-1}, Table 1). Therefore, the calculations indicate that the presence of the unreacted oxygen adsorbed near the NCO produces a displacement of the stretching frequencies to higher values, in qualitative agreement with observations. It is interesting to mention that while the internal geometry of the NCO species is essentially the same with or without preadsorbed O, the N–Cu distance is about 0.01 Å longer.

As we have already discussed, it is unlikely that the complete saturation of NCO can be reached because of the very strong intermolecular interaction. For this reason, apart from the extreme case of complete coverage, we consider another hypothetical situation wherein isocyanates are interacting among themselves, having at the same time the possibility to move to adjacent vacant sites

We thus evaluate the adsorption of four NCO on bridge sites on a large (4×4) supercell of Cu(100), giving a global coverage of 0.25 ML (Fig. 6). These NCO species form tiny islands wherein each NCO has two nearby NCO at 2.574 Å (the optimized Cu–Cu distance) as initial geometry. After geometrical optimization, the N–N distance increases up to 3.384 Å. Besides, due to intensive dipole–dipole interactions, the isocyanate ends in a tilted position with respect to the surface and bonded on pseudo-bridge sites. This process, from the initial (non-minimum) to the final relaxed geometry, is accompanied by an energy decrease of 0.84 eV per NCO. The final adsorption energy resulted to be −3.18 eV, which is only 0.19 eV less stable than the NCO adsorbed on bridge site at θ = 0.25 ML according to the p(2×2) array (Table 1). On Pd(100), the d(N–N) changes from 2.800 Å (NCO fixed on bridge sites) to 3.281 Å, with an energy diminution of 0.32 eV per NCO. However, in this case NCO species retain the perpendicularity with respect to the surface owing to the more open structure of Pd(100). The binding energy was −2.71 eV, which is 0.19 eV less stable with respect to the same coverage (θ = 0.25 ML according to the p(2×2) structure). Therefore, when NCO is located on first vicinal sites, they undergo a very strong dipole–dipole repulsive interaction on both Cu

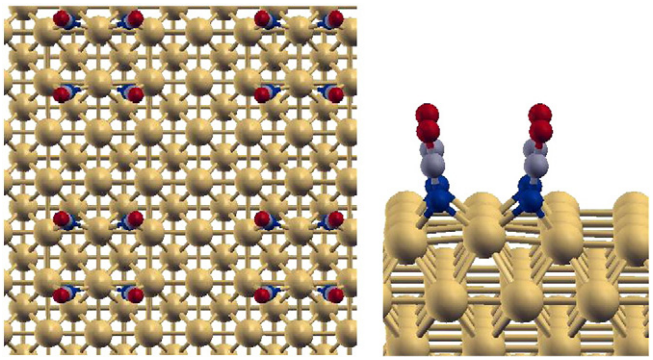

Fig. 6. Optimized geometry of four NCO species forming islands on a (4×4) supercell of Cu(100).

(100) and Pd(100) surfaces and they tend to separate to diminish this repulsion.

As previously mentioned, NCO is stable up to 500 K on the Cu(100) surface [7]. On Pd(100), the decomposition temperature is much lower [8–10]. At a first sight, according to our calculations, an easier dissociation is expected for Cu(100) than on Pd(100) because in the latter case the N–C bond is stronger owing mainly to the larger amount of charge taking by the 2π MO (with N-C bonding character). However, the experimental evidence indicates the opposite situation. With the purpose to clarify this point, we computed the energy changes associated to the NCO dissociation toward N and CO on both Cu(100) and Pd(100). For that, we calculated the energy of the final geometry after dissociation, i.e., with N and CO adsorbed on hollow sites as independent species at $\theta = 0.5$ (Fig. 7) and 0.25 ML. Afterwards, we compare the energy of these final structures with the total energies of the NCO adsorption on hollow (the initial geometries before dissociation). We found that for Cu(100), the NCO dissociation corresponds to an endothermic process and hence this energy difference is the minimal energy barrier. At 0.5 ML of NCO on Cu(100) the minimal energy barrier resulted to be 1.58 eV. We interestingly found that the final dissociative geometry has the N adatom hardly above the metal face (about 0.2 Å above the Cu surface, with a short N–Cu distance of 1.831 Å), while the CO is physisorbed with a long C–Cu distance of 3.607 Å (Fig. 7). In agreement with our result, previous theoretical calculations show that the nitrogen atom was adsorbed on Cu(100) according to the c(2×2) array with a short N–Cu bond length of 1.83 Å [31]. On the other hand, the same situation was evaluated at 0.25 ML of NCO on Cu(100) as initial structure. In the final state, N and CO are independently adsorbed covering both species half of the surface. In this case the minimal energy barrier is somewhat lower, 1.42 eV. At the dissociative state, the N–Cu distance is similar as before, 1.890 Å, but the CO is now adsorbed with a shorter C–Cu distance of 2.041 Å. Comparing both situations at these two coverages, we can note that the adsorbed N is always close to the Cu surface but the position of CO changes notably; however, the minimal barrier are similar in both cases probably due to the relatively weak interaction between CO and Cu [38]. In the case of Pd(100), starting from a NCO coverage of 0.5 ML the dissociation is also endothermic with a minimal barrier of 0.92 eV. Conversely to the case of Cu(100), the CO molecule is close to the surface in the final dissociative state (C and Pd atoms are separated by about 2.34 Å). At 0.25 ML of NCO on Pd(100), the process becomes exothermic in −0.37 eV with a C–Pd distance of 2.225 Å. In conclusion, the calculated minimal energy barriers indicate a higher tendency to dissociate on Pd(100) than on Cu(100), in agreement with experiments.

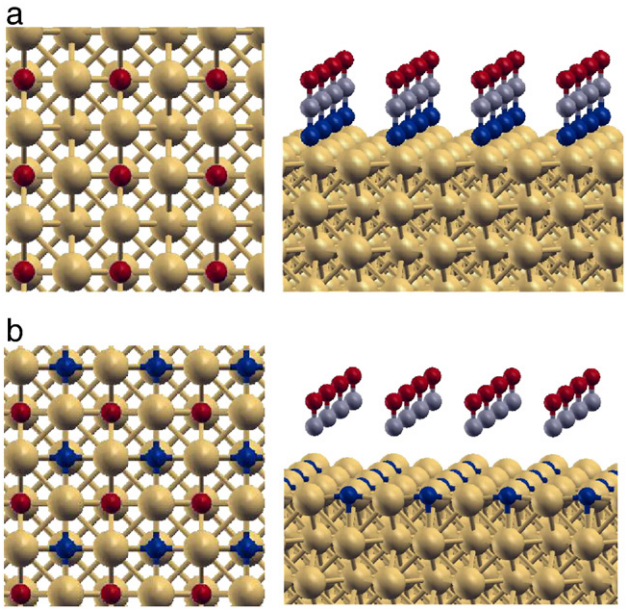

Fig. 7. (a) Top and side views of NCO adsorption on Cu(100) at hollow sites ($\theta = 0.5$). (b) Top and side views of the dissociated structure with N and CO both at hollow sites.

4. Conclusion

Our DFT calculations show that NCO adsorbs preferentially on high coordination sites (bridge and hollow) irrespective of the coverage, excepting at $\theta = 1.0$. For each site, the adsorption energy values have a nearly constant value up to 0.5 ML. The calculated positive values of $\Delta\mu$ indicate the direction of the electronic transfer: from Cu to NCO. For each value of coverage (excepting the complete saturation) both $\Delta\mu$ and $\Delta\Phi$ values indicate that the magnitude of negative charge follows the order top>bridge>hollow.

For the three adsorption sites, $\Delta\Phi$ values show an increasing behavior from $\theta = 0.11$ to 0.5. For the hollow site, a linear dependence along the whole studied range is observed. In this case, the successive incorporation of NCO increases the density of the induced dipoles and consequently $\Delta\Phi$ becomes a linear function of the coverage. For top and bridge sites, the dipole–dipole interaction produces an increasing depolarization effect as the coverage increases. The same general behavior was previously reported for NCO/Pd(100) but in this case the adsorbate–substrate electronic charge transfer is larger than on Cu(100).

At complete coverage, the Cu(100)–NCO interaction undergoes a destabilization in the range of 1.7–2.0 eV with respect to the adsorption at low coverage owing to intensive dipole–dipole interaction among surface NCO. The resulting general tendency of the NCO species is to be separated from each other generating the vacant sites required for the dissociation toward N and CO. This vacant site requirement for NCO dissociation has been suggested in the past from experiments performed on Pd(100), Pt(100) and Rh(111).

We finally found that, from a thermodynamic point of view, the NCO is more stable on Cu(100) than on Pd(100), in accord with the experimental evidences. Indeed, starting from NCO coverages of 0.25 or 0.5 ML on Cu(100) and ending with N and CO independently adsorbed, the process resulted to be endothermic with a calculated minimal barrier of about 1.5 eV. Conversely, on Pd(100) the minimal barrier decreases to about 0.9 eV at higher coverages and becomes slightly exothermic at lower ones.

Acknowledgments

This research was carried out for the financial support of CONICET, ANPCYT and Universidad Nacional del Sur.

References

[1] F. Solymosi, L. Völgyesi, J. Sárkány, J. Catal. 54 (1978) 336.
[2] W.C. Hecker, A.T. Bell, J. Catal. 85 (1984) 389.
[3] F. Solymosi, T. Bánsági, J. Catal. 156 (1995) 75.
[4] J.E. Jones, M. Trenary, J. Phys. Chem. C 112 (2008) 20443.
[5] C. Neyertz, M. Volpe, D. Costilla, M. Sánchez, C. Gígola, Appl. Catal. A General 368 (2009) 146.
[6] F. Solymosi, J. Kiss, Surf. Sci. 104 (1981) 181.
[7] H. Celio, K. Mudalige, P. Mills, M. Trenary, Surf. Sci. 394 (1997) L168.
[8] R. Németh, J. Kiss, F. Solymosi, J. Phys. Chem. C 111 (2007) 1424.
[9] R.J. Gorte, L.D. Schmidt, B.A. Sexton, J. Catal. 67 (1981) 387.
[10] F. Solymosi, J. Kiss, Surf. Sci. 108 (1981) 641.
[11] H. Yang, J.L. Whitten, Surf. Sci. 401 (1998) 312.
[12] G.R. Garda, R.M. Ferullo, N.J. Castellani, Surf. Rev. Lett. 8 (2001) 641.
[13] G.R. Garda, R.M. Ferullo, N.J. Castellani, Surf. Sci. 598 (2005) 57.
[14] J.M. Hu, Y. Li, J.Q. Li, Y.F. Zhang, W. Lin, G.X.J. Jia, Solid State Chem. 177 (2004) 2763.
[15] P.G. Belelli, M.M. Branda, G.R. Garda, R.M. Ferullo, N.J. Castellani, Surf. Sci. 604 (2010) 442.
[16] S. Zhao, Y. Ren, J. Wang, W. Yin, J. Phys. Chem. A 113 (2009) 1075.
[17] R.M. Ferullo, N.J. Castellani, J. Mol. Catal. A 221 (2004) 155.
[18] J. Kiss, F. Solymosi, J. Catal. 179 (1998) 277.
[19] G. Kresse, J. Hafner, Phys. Rev. B 47 (1993) 558.
[20] G. Kresse, J. Hafner, Phys. Rev. B 48 (1993) 13115.
[21] G. Kresse, J. Hafner, Phys. Rev. B 49 (1994) 14251.
[22] P. Blochl, Phys. Rev. B 50 (1994) 17953.
[23] G. Kresse, D. Joubert, Phys. Rev. B 59 (1999) 1758.
[24] J.P. Perdew, J.A. Chevary, S.H. Vosko, K.A. Jackson, M.R. Pederson, D.J. Singh, C. Fiolhais, Phys. Rev. B 46 (1992) 6671.
[25] J.P. Perdew, J.A. Chevary, S.H. Vosko, K.A. Jackson, M.R. Pederson, D.J. Singh, C. Fiolhais, Phys. Rev. B 48 (1993) 4978.
[26] H.J. Monkhorst, J.D. Pack, Phys. Rev. B 13 (1976) 5188.
[27] M. Methfessel, A.T. Paxton, Phys. Rev. B 40 (1989) 3616.
[28] Ch. Kittel, Introduction to Solid State Physics, 7th ed. John Wiley and Sons, Inc., New York, 1996.
[29] J.L.F. Da Silva, K. Schroeder, S. Blügel, Phys. Rev. B 69 (2004) 245411.
[30] S.B. Sinnott, M.S. Stave, T.J. Raeker, A.E. DePristo, Phys. Rev. B 16 (1991) 8927.
[31] X.-M. Tao, M.-Q. Tan, X.-X. Zhao, W.-B. Chen, X. Chen, X.-F. Shang, Surf. Sci. 600 (2006) 3419.
[32] X. Duan, O. Warschkow, A. Soon, B. Delley, C. Stampfl, Phys. Rev. B 81 (2010) 075430.
[33] R. Mayer, Ch-S. Zhang, K.G. Lynn, W.E. Frieze, F. Jona, P.M. Marcus, Phys. Rev. B 35 (1987) 3102.
[34] D.M. Lind, F.B. Dunning, G.K. Walters, H.L. Davis, Phys. Rev. B 35 (1987) 9037.
[35] A.P. Scott, L. Radom, J. Phys. Chem. 100 (1996) 16502.
[36] K.N. Wong, W.R. Anderson, A.J. Kotlar, J.A. Vanderhoff, J. Chem. Phys. 81 (1984) 2970.
[37] H.B. Michaelson, J. Appl. Phys. 48 (1977) 4729.
[38] C.M. Truong, J.A. Rodríguez, D.W. Goodman, Surf. Sci. Lett. 271 (1992) L385.